The *OsSPL16-GW7* regulatory module determines grain shape and simultaneously improves rice yield and grain quality

Shaokui Wang[1,2], Shan Li[1], Qian Liu[1], Kun Wu[1], Jianqing Zhang[1], Shuansuo Wang[1], Yi Wang[1], Xiangbin Chen[1], Yi Zhang[1], Caixia Gao[1], Feng Wang[3], Haixiang Huang[4] & Xiangdong Fu[1]

The deployment of heterosis in the form of hybrid rice varieties has boosted grain yield, but grain quality improvement still remains a challenge. Here we show that a quantitative trait locus for rice grain quality, *qGW7*, reflects allelic variation of *GW7*, a gene encoding a TONNEAU1-recruiting motif protein with similarity to C-terminal motifs of the human centrosomal protein CAP350. Upregulation of *GW7* expression was correlated with the production of more slender grains, as a result of increased cell division in the longitudinal direction and decreased cell division in the transverse direction. OsSPL16 (GW8), an SBP-domain transcription factor that regulates grain width, bound directly to the *GW7* promoter and repressed its expression. The presence of a semidominant *GW7*[TFA] allele from tropical *japonica* rice was associated with higher grain quality without the yield penalty imposed by the Basmati *gw8* allele. Manipulation of the *OsSPL16-GW7* module thus represents a new strategy to simultaneously improve rice yield and grain quality.

Over the past 50 years, the two most substantial contributions to rice yield have been increased harvest index (the proportion of a plant's aerial biomass that is represented by grain), achieved by deploying semidwarfness[1,2], and the exploitation of heterosis[3,4]. However, improvements in grain quality still remains a major problem[5], as this trait is a complex trait that is multiplicatively determined by appearance, cooking and eating quality, etc., all of which are controlled by quantitative trait loci (QTLs) and influenced by environmental changes. Despite a great deal of research effort[6–10], only a small number of relevant genes have been identified thus far[11–13].

Shanyou63 is the most widely grown hybrid variety in China. Its parents are the restorer line Mnghui63 (MH63) and the cytoplasmic male sterility (CMS) line Zhenshan97A (ZS97A). Its grains are short and wide and are considered to be of only mediocre quality (**Fig. 1a,b** and **Supplementary Fig. 1**). In contrast, the hybrid formed by crossing MH63 and the newly developed CMS line TaifengA (TFA) produces long, slender grains with excellent quality (**Fig. 1a,b** and **Supplementary Table 1**). The two hybrids differ only marginally from one another with respect to grain yield components (**Supplementary Fig. 2**). To investigate the genetic basis of improved grain quality, we used an F_2 population of 400 individuals developed from a cross between 2 maintainer lines (ZS97B and TFB) and identified 2 major grain width QTLs, termed *qGW4* and *qGW7*, along with 3 major grain length QTLs (*qGL3*, *qGL7* and *qGL12*) (**Fig. 1c**). Cosegregation in the BC_1F_2 generation derived from the backcross between TFB and ZS97B (with ZS97B as the recurrent parent) suggested that *qGL3* mapped to the same locus as *qGS3*, and sequence comparison showed that TFA and TFB had the same loss-of-function *gs3* allele as MH63 (ref. 14 and data not shown). Both *qGW7* and *qGL7* mapped to the same region of chromosome 7 (**Fig. 1c**). Further genetic analysis of a BC_2F_2 population suggested that a semidominant *qGW7* allele from TFB was responsible for grain slenderness (**Supplementary Fig. 3**).

Fine-scale mapping of *qGW7* using 4,500 BC_3F_2 plants bred from the backcross between TFA and HJX74 (with HJX74 as the recurrent parent) allowed the position of the locus to be confined to a ~20-kb segment flanked by markers M1 and M10 (**Fig. 1d**). A progeny test of homozygous segregants further narrowed the interval to a ~2.6-kb region flanked by markers S5 and S6 (**Fig. 1e**); this stretch of DNA harbors the promoter region and exon 1 of the *LOC_Os07g41200* gene (**Fig. 1f**), hereafter referred to as *GW7*. The *GW7* gene encodes a homolog of the *Arabidopsis thaliana* TONNEAU1 (TON1 (ref. 15))-recruiting motif (TRM) proteins[16] (**Supplementary Fig. 4**), and the encoded GW7 also shows homology to C-terminal motifs in the human centrosomal protein CAP350 (**Supplementary Fig. 5**)[16,17]. Sequence analysis showed that a set of 18 SNPs and 9 indels in the promoter region of *GW7* differed between TFA and HJX74 (**Fig. 1f** and **Supplementary Table 2**).

The near-isogenic line NIL-*GW7*[TFA] is homozygous for the TFA *qGW7* allele on an *indica* HJX74 background, whereas NIL-*gw7*[HJX74] is homozygous for the HJX74 allele. We compared the transcript levels

Figure 1 Positional cloning of *qGW7*. (**a**) Grains from the parents of *indica* hybrid rice lines. Scale bar, 2 mm. (**b**) Grain chalkiness of the two hybrid combinations (ZS97A × MH63 and TFA × MH63). (**c**) QTL locations for grain width and grain length. LOD, logarithm of odds. (**d**) *qGW7* was mapped to a ~20-kb genomic DNA region between markers M1 and M10 using 4,500 BC_3F_2 plants. The numbers below the bar indicate the number of recombinants between *qGW7* and the molecular markers shown. (**e**) Genotyping of progeny homozygous for *qGW7* delimited the locus to a ~2.6-kb stretch flanked by markers S5 and S6. Grain width is shown for recombinant BC_4F_3 plants (L1–L4) and the parental plant. Filled and open bars represent chromosomal segments homozygous for, respectively, the TFA and HJX74 alleles. Data are shown as means ± s.e.m. (*n* = 60). (**f**) Allelic variation in the candidate gene *LOC_Os07g41200* (*GW7*) between TFA and HJX74.
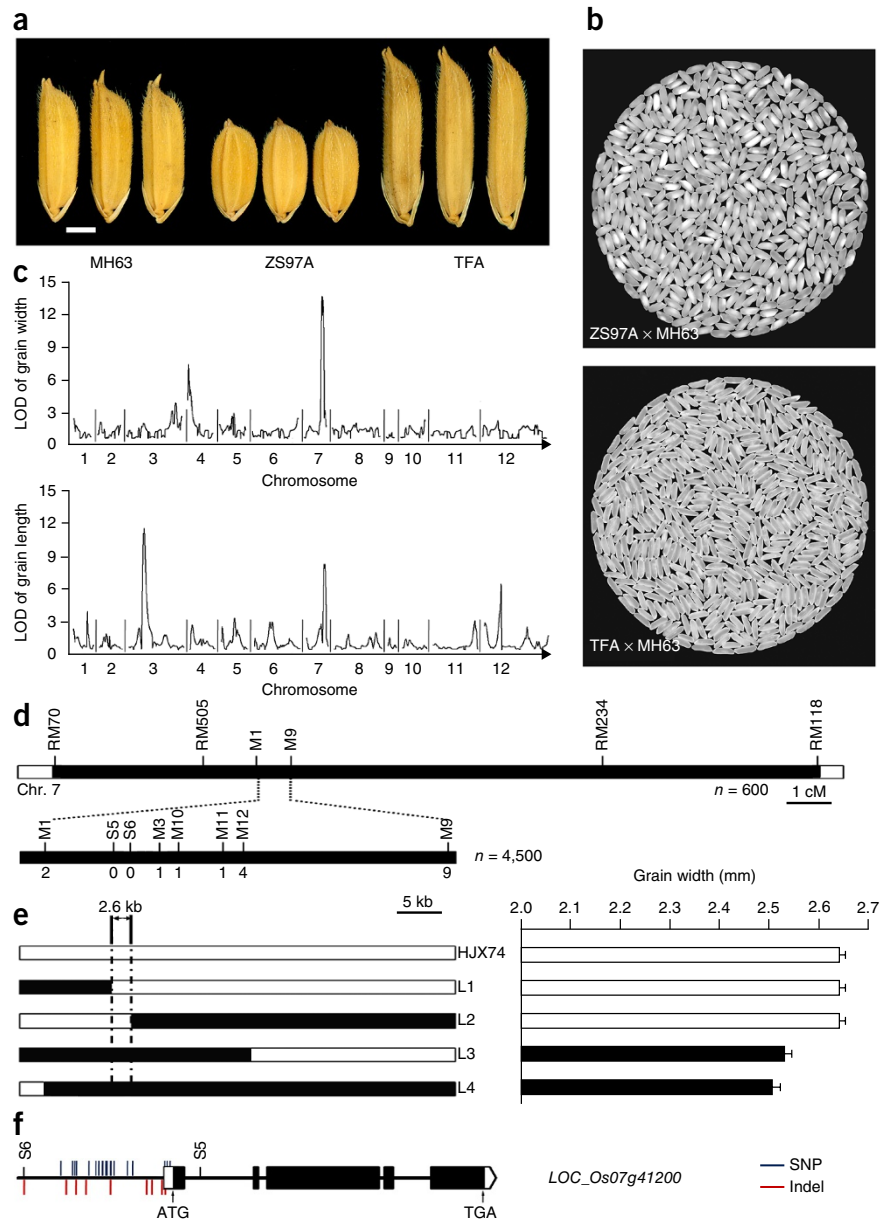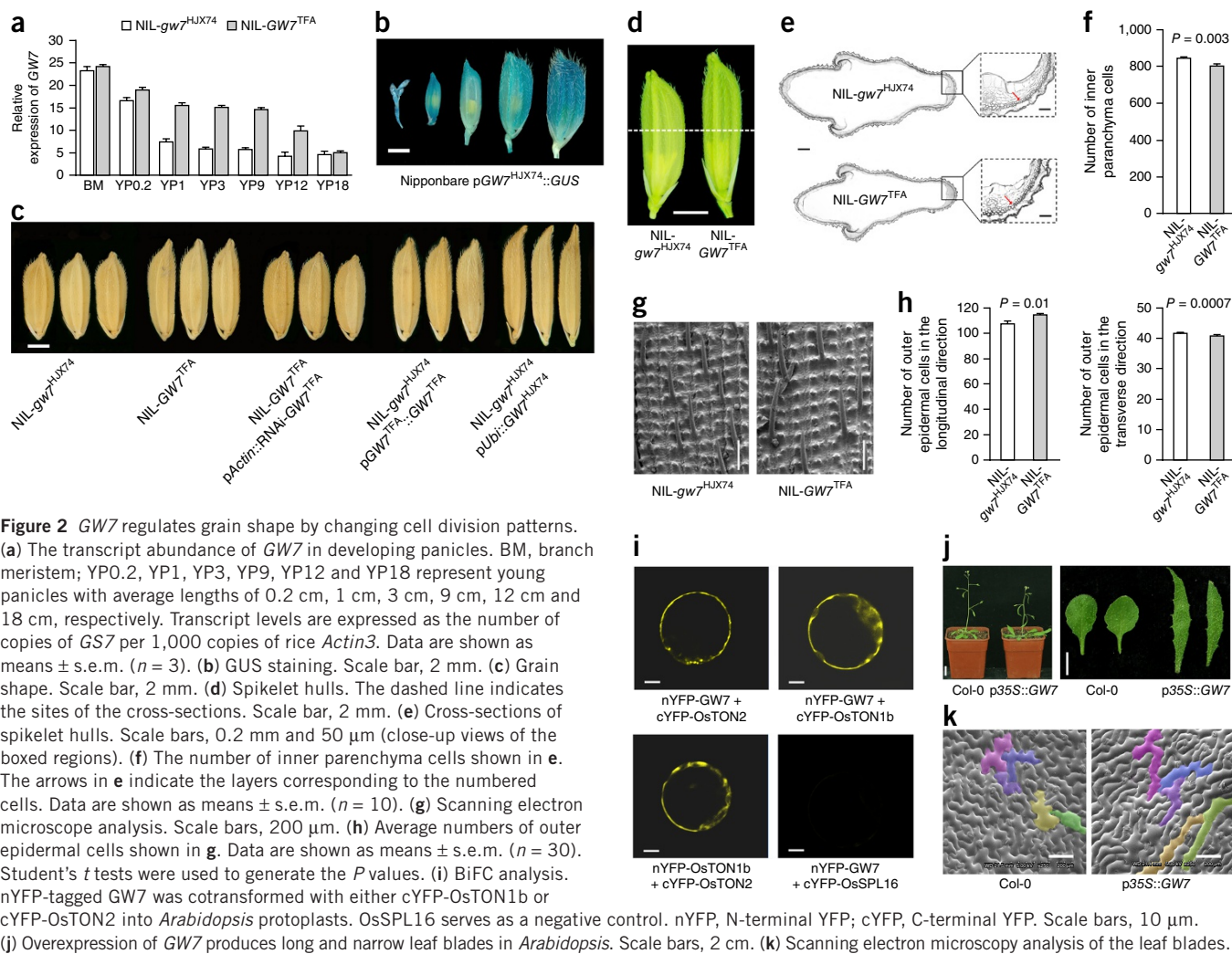

of *GW7* in various organs during vegetative growth, reproductive development[18,19] and the development of rice endosperms (**Fig. 2a** and **Supplementary Figs. 6** and **7**). Quantitative RT-PCR (qRT-PCR) analysis identified differences in *GW7* transcript abundance between NIL-*GW7*[TFA] and NIL-*gw7*[HJX74], with the gene being transcribed more strongly in NIL-*GW7*[TFA] than in NIL-*gw7*[HJX74] during panicle development (**Fig. 2a**) and in the middle stages of rice endosperm development (**Supplementary Fig. 7**). Transgenic plants carrying a p*GW7*[HJX74]∷*GUS* construct (with the *GUS* reporter gene under the control of the *GW7* promoter from HJX74) showed a strong GUS signal in spikelet hulls (**Fig. 2b**). NIL-*gw7*[HJX74] plants transgenic for the TFA *GW7* cDNA whose expression was driven by its native promoter produced more slender grains than those formed for non-transgenic NIL-*gw7*[HJX74] plants (**Fig. 2c**). Conversely, Transgenic NIL-*GW7*[TFA] plants that underwent RNA interference (RNAi)-mediated silencing of *GW7* formed shorter and wider grains than those formed by non-transgenic NIL-*GW7*[TFA] plants (**Fig. 2c**). Transgenic NIL-*gw7*[HJX74] plants in which the HJX74 *GW7* cDNA was constitutively overexpressed formed grains that were substantially narrower and longer than those formed by non-transgenic NIL-*GW7*[TFA] plants (**Fig. 2c**). These results indicate that upregulation of *GW7* promotes the formation of more slender grains.

Before fertilization, the spikelet hulls formed by NIL-*gw7*[HJX74] plants were shorter and wider than those formed by NIL-*GW7*[TFA] plants (**Fig. 2d**). An inspection of palea and lemma transverse sections showed that there were fewer inner parenchyma cells in NIL-*GW7*[TFA] than in NIL-*gw7*[HJX74] (**Fig. 2e**,**f**). The average width of NIL-*GW7*[TFA] outer epidermal cells was slightly greater than that for NIL-*gw7*[HJX74] cells (**Fig. 2g** and **Supplementary Fig. 8a**), but there was a ~6.4% decrease in transverse cell proliferation in NIL-*GW7*[TFA] spikelet hulls (**Fig. 2h**), indicating that the reduced grain width in NIL-*GW7*[TFA] results from decreased cell division in the transverse direction. Conversely, the average length of the NIL-*GW7*[TFA] outer

epidermal cells was indistinguishable from that of NIL-*gw7*[HJX74] cells (**Fig. 2g** and **Supplementary Fig. 8b**), whereas there was a ~6.5% increase in longitudinal cell proliferation in NIL-*GW7*[TFA] spikelet hulls (**Fig. 2h**). The implication of these findings is that the formation of slender grains results from increased cell division in the longitudinal direction and decreased cell division in the transverse direction. Thus, *GW7* appears to regulate grain shape by changing cell division patterns.

We next screened for GW7-interacting proteins by yeast two-hybrid assay with GW7 as bait and identified 18 candidates (**Supplementary Table 3**), including a rice homolog of TON1 (LOC_Os11g01170, hereafter OsTON1b) and a homolog of PP2A (also known as FASS or TON2; LOC_Os05g05710, hereafter OsTON2))[20]. In *Arabidopsis*, TRM1, which is synonymous with LONGIFOLIA2 (LNG2)[21], has been identified as targeting TON1, a protein that is similar to the human centrosomal protein FOP[22], to cortical microtubules[16,17]. Recently, a TTP (TON1-TRM-PP2A) protein complex has been described to be involved in preprophase band formation and the
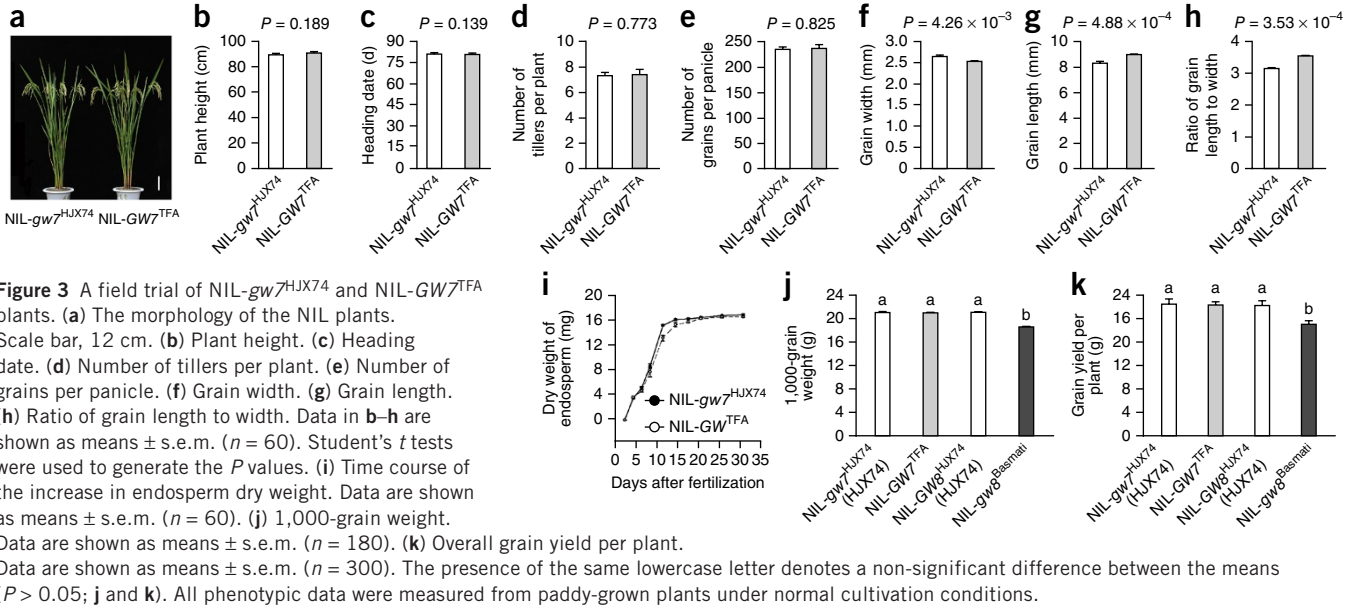
Figure 2 *GW7* regulates grain shape by changing cell division patterns. (**a**) The transcript abundance of *GW7* in developing panicles. BM, branch meristem; YP0.2, YP1, YP3, YP9, YP12 and YP18 represent young panicles with average lengths of 0.2 cm, 1 cm, 3 cm, 9 cm, 12 cm and 18 cm, respectively. Transcript levels are expressed as the number of copies of *GS7* per 1,000 copies of rice *Actin3*. Data are shown as means ± s.e.m. (*n* = 3). (**b**) GUS staining. Scale bar, 2 mm. (**c**) Grain shape. Scale bar, 2 mm. (**d**) Spikelet hulls. The dashed line indicates the sites of the cross-sections. Scale bar, 2 mm. (**e**) Cross-sections of spikelet hulls. Scale bars, 0.2 mm and 50 µm (close-up views of the boxed regions). (**f**) The number of inner parenchyma cells shown in **e**. The arrows in **e** indicate the layers corresponding to the numbered cells. Data are shown as means ± s.e.m. (*n* = 10). (**g**) Scanning electron microscope analysis. Scale bars, 200 µm. (**h**) Average numbers of outer epidermal cells shown in **g**. Data are shown as means ± s.e.m. (*n* = 30). Student's *t* tests were used to generate the *P* values. (**i**) BiFC analysis. nYFP-tagged GW7 was cotransformed with either cYFP-OsTON1b or cYFP-OsTON2 into *Arabidopsis* protoplasts. OsSPL16 serves as a negative control. nYFP, N-terminal YFP; cYFP, C-terminal YFP. Scale bars, 10 µm. (**j**) Overexpression of *GW7* produces long and narrow leaf blades in *Arabidopsis*. Scale bars, 2 cm. (**k**) Scanning electron microscopy analysis of the leaf blades.

spatial control of cell division in plants[23]. Bimolecular fluorescence complementation (BiFC) assays showed that GW7 could interact with both OsTON2 and OsTON1b and that OsTON2 also interacted with OsTON1b (**Fig. 2i**). Similarly to the *Arabidopsis* TTP protein complex, the M2 and M3 motifs of GW7 were involved in interaction with OsTON1b and OsTON2, respectively (**Supplementary Fig. 9**), suggesting that interactions within the TTP complex are conserved between *Arabidopsis* and rice. Moreover, transgenic *Arabidopsis* plants constitutively overexpressing TFA *GW7* cDNA under the control of the cauliflower mosaic virus (CaMV) *35S* promoter had increased longitudinal polar cell elongation, as manifested by long and narrow leaf blades (**Fig. 2j,k**), a phenotype that was indistinguishable from those of p*35S*∷*LNG1* and p*35S*∷*LNG2* plants[21].

We quantified the effect of allelic variation at the *GW7* locus on rice yield and grain quality in a field trial of NIL-*gw7*[HJX74] and NIL-*GW7*[TFA] plants grown under normal cultivation conditions[12,24]. The two NILs did not differ from one another with respect to heading date, plant height, the number of tillers per plant and the number of grains per panicle (**Fig. 3a**–**e**), but their grain shapes were clearly distinct (**Fig. 3f**–**h**). The width of the NIL-*GW7*[TFA] grain was ~6.0% less and its length was ~5.9% greater in comparison to NIL-*gw7*[HJX74] grain, resulting in the formation of a more slender grain (**Figs. 2c** and **3h**). Upregulation of *GW7* slightly decreased the grain-filling rate (**Fig. 3i**), increased the transcript levels of several starch synthesis genes in

developing rice endosperms (**Supplementary Fig. 10**) and substantially enhanced rice grain appearance quality (**Supplementary Table 4**), consistent with the observed improvement of rice endosperm chalkiness (**Supplementary Fig. 11**). It has been reported previously that the *gw8*[Basmati] allele found in Basmati rice, encoding the SBP (SQUAMOSA PROMOTER–BINDING PROTEIN)-domain transcription factor OsSPL16, is associated with the formation of more slender grains and better grain quality[12], but this allele is also associated with a ~14% penalty in grain yield (**Fig. 3j,k**). In contrast, there was little difference between NIL-*gw7*[HJX74] and NIL-*GW7*[TFA] plants with respect to grain weight and overall grain yield per plant (**Fig. 3j,k**). These results indicate that the semidominant *GW7*[TFA] allele is associated with the formation of more slender grains and better quality as well as the advantage in grain yield over the Basmati *gw8* allele.

The transcript abundance of *GW7* in NIL-*gw8*[Basmati] increased over the course of panicle development when compared to NIL-*GW8*[HJX74], whereas *GW7* expression was substantially reduced in transgenic NIL-*gw8*[Basmati] plants that had upregulation of *OsSPL16* or RNAi-mediated silencing of *GW7* (**Fig. 4a**), suggesting that *GW7* expression is negatively regulated by OsSPL16. Furthermore, transgenic NIL-*gw8*[Basmati] plants with either upregulation of *OsSPL16* or downregulation of *GW7* formed wider and shorter grains than those formed by non-transgenic NIL-*gw8*[Basmati] plants (**Fig. 4b**). The inference

Figure 3 A field trial of NIL-$gw7^{HJX74}$ and NIL-$GW7^{TFA}$ plants. (**a**) The morphology of the NIL plants. Scale bar, 12 cm. (**b**) Plant height. (**c**) Heading date. (**d**) Number of tillers per plant. (**e**) Number of grains per panicle. (**f**) Grain width. (**g**) Grain length. (**h**) Ratio of grain length to width. Data in **b**–**h** are shown as means ± s.e.m. ($n = 60$). Student's t tests were used to generate the P values. (**i**) Time course of the increase in endosperm dry weight. Data are shown as means ± s.e.m. ($n = 60$). (**j**) 1,000-grain weight. Data are shown as means ± s.e.m. ($n = 180$). (**k**) Overall grain yield per plant. Data are shown as means ± s.e.m. ($n = 300$). The presence of the same lowercase letter denotes a non-significant difference between the means ($P > 0.05$; **j** and **k**). All phenotypic data were measured from paddy-grown plants under normal cultivation conditions.

from these findings is that *GW7* must act downstream of *OsSPL16*. Chromatin immunoprecipitation (ChIP) and electrophoretic mobility shift assay (EMSA) analyses demonstrated that OsSPL16 was able to bind the *GW7* promoter *in vivo* and *in vitro* (**Fig. 4c,d**). Further EMSA experiments showed that OsSPL16 was able to bind the GTAC[25] motifs of the F8 fragment in the promoter

Figure 4 OsSPL16 negatively regulates *GW7* expression. (**a**) Transcript levels for *GW7* in young panicles. Expression is shown relative to that of NIL-$GW8^{HJX74}$ plants, which was set to 1. Data are shown as means ± s.e.m. ($n = 3$). (**b**) Grain shape. Scale bar, 2 mm. (**c**) ChIP assays. The diagram depicts the regions used for ChIP-PCR analysis of extracts from young panicles of NIL-$gw8^{Basmati}$ plants carrying the p*Actin*::*Myc-OsSPL16* construct. ChIP-PCR results were quantified by normalization of the Myc immunoprecipitation signal by the corresponding input signal. Data are shown as means ± s.e.m. ($n = 3$). (**d**) EMSA analysis. Competition for OsSPL16 binding was performed with cold probe containing the GTAC motifs at 10×, 20×, 30× and 50× the amount of labeled probe. (**e**) OsSPL16 represses transcription of the *GW7* gene promoter. Relative luciferase activity was monitored in rice protoplasts cotransfected with different effector and reporter constructs. Mock, cotransfected with reporter construct and an empty effector construct; control, cotransfected with effector construct and an empty reporter construct (set to 1). Data are shown as means ± s.e.m. ($n = 3$). Student's t tests were used to generate the P values. (**f**) Variations in the F8 fragment between the HJX74 and TFA alleles. The red box highlights the GTAC motifs. (**g**) Yeast one-hybrid assays. The 0.5-kb and 1.0-kb DNA fragments upstream of the *GW7* transcription start site were used to construct *lacZ* expression vectors[32]. Data are shown as means ± s.e.m. ($n = 3$). The pB42AD and pLacZi2μ empty vectors, pB42AD::*OsSPL16* and the pLacZi2μ empty vector, and p*gw7*$^{HJX74 (1.0 kb)}$::*lacZ* and the

pB42AD empty vector were used as the negative control (control 1), control 2 and control 3, respectively. The presence of the same lowercase letter denotes a non-significant difference between the means ($P > 0.05$).
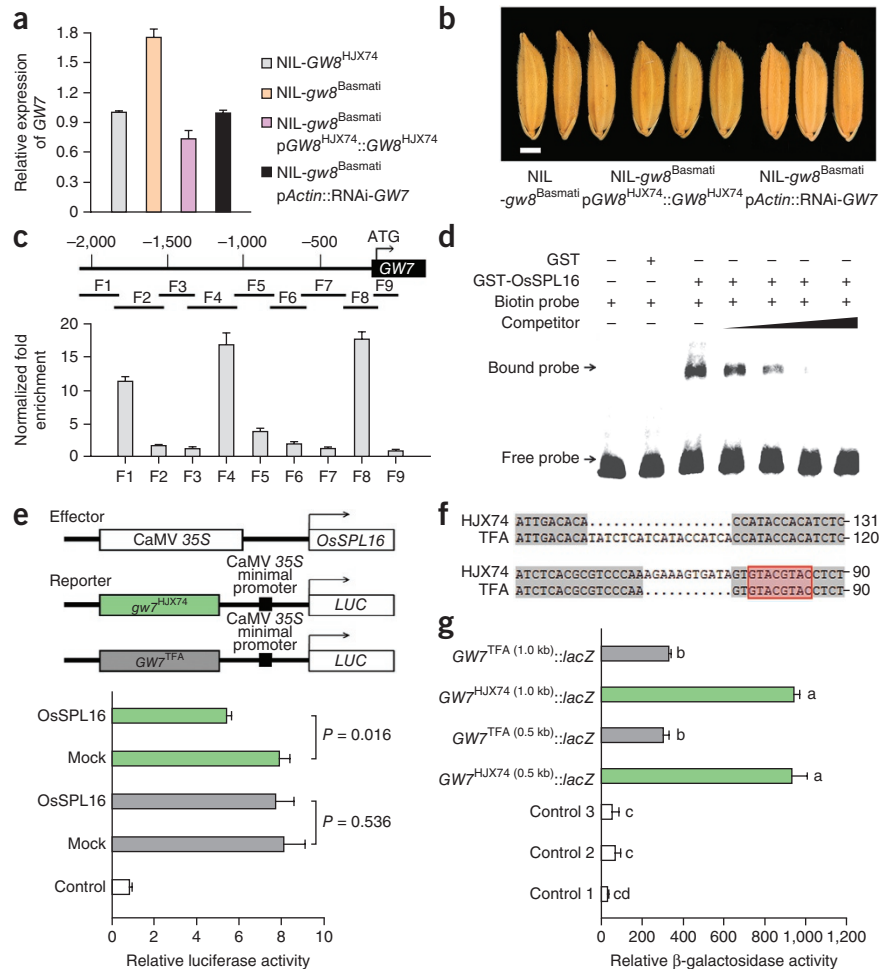
Table 1 Pyramiding of the $GW7^{TFA}$ and $gs3$ alleles enhances grain yield

Trait	NIL-$GS3$-$gw7^{HJX74}$	NIL-$GS3$-$GW7^{TFA}$	NIL-$gs3$-$gw7^{HJX74}$	NIL-$gs3$-$GW7^{TFA}$
Plant height (cm)	90.41 ± 0.63[a]	91.50 ± 0.73[a,b]	90.21 ± 0.62[a]	91.92 ± 0.52[a,b]
Tiller numbers per plant	7.25 ± 0.26[c]	7.30 ± 0.25[c]	6.95 ± 0.29[c]	7.26 ± 0.24[c]
Panicle length (cm)	20.63 ± 0.17[d]	20.96 ± 0.20[d]	21.11 ± 0.36[d]	21.04 ± 0.28[d]
Grain number per panicle	222.30 ± 7.30[e]	225.50 ± 6.57[e]	213.22 ± 4.91[e,f]	207.00 ± 5.13[f]
1,000-grain weight (g)	21.27 ± 0.02[d]	21.21 ± 0.05[d]	22.31 ± 0.07[g]	25.00 ± 0.05[h]
Actual yield per plot (g)	1,151.65 ± 30.24[i]	1,154.40 ± 19.86[i]	1,164.79 ± 9.59[j]	1,296.61 ± 34.12[k]

All phenotypic data were obtained from paddy-grown NIL plants, which were planted in a randomized block design with three replications under normal cultivation conditions. Data are shown as means ± s.e.m. estimated from 30 plots (each plot contained 50 plants). The presence of the same lowercase letter denotes a non-significant difference between the means ($P > 0.05$).

region of $GW7$, whereas mutations of GTAC to ATAC abolished its affinity (**Supplementary Fig. 12**).

We further used the rice protoplast transient expression assay system to analyze the effect of $OsSPL16$ on the expression of a reporter construct containing the 2-kb $GW7$ promoter fragment fused with the firefly luciferase coding sequence (LUC). We could detect luciferase activity in the cells expressing p$GW7^{HJX74}$::LUC, but coexpression of p$GW7^{HJX74}$::LUC with the p$35S$::$OsSPL16$ construct led to a reduction in luciferase activity (**Fig. 4e**), indicating that OsSPL16 functions as a transcriptional repressor. In contrast, ectopic expression of $OsSPL16$ did not effectively repress p$GW7^{TFA}$::LUC expression in the transient expression assay (**Fig. 4e**). Among the three binding sites for OsSPL16 in the $GW7$ promoter (**Fig. 4c**), the GTAC motifs in the $GW7^{TFA}$ allele were in close proximity to an 11-bp deletion and 18-bp insertion located in the F8 fragment (**Fig. 4f**), and yeast one-hybrid assays demonstrated that these variations were associated with the binding activity of OsSPL16 to the $GW7$ promoter (**Fig. 4g** and **Supplementary Fig. 13**). Although the $gw8^{Basmati}$ allele resulted in the upregulation of $GW7$ (**Fig. 4a**), the size and shape of the grains produced by NIL-$GW7^{TFA}$-$gw8^{Basmati}$ plants were similar to those for grains formed by NIL-$GW7^{TFA}$-$GW8^{HJX74}$ plants (**Supplementary Fig. 14**). These results suggest that OsSPL16 controls grain shape via repression of $GW7$.

Pedigree records show that TFA and TFB were derived from the tropical *japonica* rice variety Mi31, and a resequencing study showed that the TFA haplotype involving an 11-bp deletion and an 18-bp insertion was common across tropical *japonica* germplasm but was unrepresented among high-yielding *indica* cultivars (**Supplementary Table 5**), indicating that this TFA haplotype has not yet been selected in *indica* rice breeding programs. The $gs3$ allele, which proved to be a major determinant of grain length in TFA (**Fig. 1c**), has been widely used in *indica* rice breeding[14]. To test the potential of combining beneficial alleles to improve grain quality and/or yield, we generated NILs carrying various combinations of alleles at the $qGS3$ and $qGW7$ loci on the HJX74 background. NIL-$gs3$-$gw7^{HJX74}$ plants formed more slender grains than those formed by NIL-$GS3$-$GW7^{TFA}$ plants, whereas NIL-$gs3$-$GW7^{TFA}$ plants produced much longer grains than either NIL-$GS3$-$GW7^{TFA}$ or NIL-$gs3$-$gw7^{HJX74}$ plants (**Supplementary Fig. 15**). Over three successive years of field trials, NIL-$gs3$-$GW7^{TFA}$ plants were ~10.7% more productive than NIL-$gs3$-$gw7^{HJX74}$ plants, whereas NIL-$gs3$-$GW7^{TFA}$ plants demonstrated a ~12.6% advantage in grain yield over HJX74 (NIL-$GS3$-$gw7^{HJX74}$) plants (**Table 1**), with substantial improvements in grain quality also being achieved (**Supplementary Table 6**). Thus, the combination of the $GW7^{TFA}$ and $gs3$ alleles provides a new strategy for simultaneously improving rice yield and grain quality over what is currently achievable. Consistent with this notion, we have used QTL pyramiding of the $GW7^{TFA}$ and $gs3$ alleles and developed new high-yielding *indica* hybrid

rice varieties (for example, Taifengyou55 and Taifengyou208) with substantially improved grain quality.

In summary, our results suggest that allelic variants of the $GW7$ gene regulate grain size and shape in rice, and our findings provide new insights into the role of SBP-domain transcription factors in the spatial control of plant cell division. The expression of $OsSPL16$ is already known to be controlled by OsmiR156 (refs. 12,26); thus, manipulation of the OsmiR156-$OsSPL16$-$GW7$ regulatory module opens the way to breeding simultaneously for higher grain yield and better grain quality in rice.

METHODS

Methods and any associated references are available in the online version of the paper.

Note: Any Supplementary Information and Source Data files are available in the online version of the paper.

AUTHOR CONTRIBUTIONS
Shaokui Wang performed most of the experiments. S.L. and F.W. conducted QTL analysis. K.W. and Y.W. developed the NILs. Y.Z. and C.G. performed rice transformation. S.L. and Q.L. analyzed genetic diversity. K.W. and H.H. analyzed grain quality. Shuansuo Wang and J.Z. performed yeast two-hybrid screening. X.C. and Shaokui Wang performed ChIP and EMSA assays. X.F. designed the experiments and wrote the manuscript. All authors have discussed the results and contributed to the drafting of the manuscript.

COMPETING FINANCIAL INTERESTS
The authors declare no competing financial interests.

Reprints and permissions information is available online at http://www.nature.com/reprints/index.html.

1. Sasaki, A. *et al.* A mutant gibberellin-synthesis gene in rice. *Nature* **416**, 701–702 (2002).
2. Spielmeyer, W., Ellis, M.H. & Chandler, P.M. Semidwarf (*sd-1*), "green revolution" rice, contains a defective gibberellin 20-oxidase gene. *Proc. Natl. Acad. Sci. USA* **99**, 9043–9048 (2002).
3. Yuan, L. Hybrid rice breeding for super high yield. *Hybrid Rice* **12**, 1–6 (1997).
4. Xing, Y. & Zhang, Q. Genetic and molecular bases of rice yield. *Annu. Rev. Plant Biol.* **61**, 421–442 (2010).
5. Tian, Z. *et al.* Allelic diversities in rice starch biosynthesis lead to a diverse array of rice eating and cooking qualities. *Proc. Natl. Acad. Sci. USA* **106**, 21760–21765 (2009).
6. Ahn, S.N., Bollich, C.N., McClung, A.M. & Tanksley, S.D. RFLP analysis of genomic regions associated with cooked-kernel elongation in rice. *Theor. Appl. Genet.* **87**, 27–32 (1993).
7. Aluko, G. *et al.* QTL mapping of grain quality traits from the interspecific cross *Oryza sativa* × *O. glaberrima*. *Theor. Appl. Genet.* **109**, 630–639 (2004).
8. Wang, L.Q. *et al.* Genetic basis of 17 traits and viscosity parameters characterizing the eating and cooking quality of rice grain. *Theor. Appl. Genet.* **115**, 463–476 (2007).

9. Zhou, L. *et al.* Fine mapping of the grain chalkiness QTL *qPGWC-7* in rice (*Oryza sativa* L.). *Theor. Appl. Genet.* **118**, 581–590 (2009).

10. Nelson, J.C. *et al.* Mapping QTL main and interaction influences on milling quality in elite US rice germplasm. *Theor. Appl. Genet.* **122**, 291–309 (2011).

11. Cai, X.L., Wang, Z.Y., Xing, Y.Y., Zhang, J.L. & Hong, M.M. Aberrant splicing of intron 1 leads to the heterogeneous 5′ UTR and decreased expression of *waxy* gene in rice cultivars of intermediate amylose content. *Plant J.* **14**, 459–465 (1998).

12. Wang, S. *et al.* Control of grain size, shape and quality by *OsSPL16* in rice. *Nat. Genet.* **44**, 950–954 (2012).

13. Li, Y. *et al. Chalk5* encodes a vacuolar H+-translocating pyrophosphatase influencing grain chalkiness in rice. *Nat. Genet.* **46**, 398–404 (2014).

14. Fan, C. *et al. GS3*, a major QTL for grain length and weight and minor QTL for grain width and thickness in rice, encodes a putative transmembrane protein. *Theor. Appl. Genet.* **112**, 1164–1171 (2006).

15. Azimzadeh, J. *et al. Arabidopsis* TONNEAU1 proteins are essential for preprophase band formation and interact with centrin. *Plant Cell* **20**, 2146–2159 (2008).

16. Drevensek, S. *et al.* The *Arabidopsis* TRM1-TON1 interaction reveals a recruitment network common to plant cortical microtubule arrays and eukaryotic centrosomes. *Plant Cell* **24**, 178–191 (2012).

17. Patel, H., Truant, R., Rachubinski, R.A. & Capone, J.P. Activity and subcellular compartmentalization of peroxisome proliferator-activated receptor α are altered by the centrosome-associated protein CAP350. *J. Cell Sci.* **118**, 175–186 (2005).

18. Shao, G. *et al.* Allelic variation for a candidate gene for *GS7*, responsible for grain shape in rice. *Theor. Appl. Genet.* **125**, 1303–1312 (2012).

19. Qiu, X., Gong, R., Tan, Y. & Yu, S. Mapping and characterization of the major quantitative trait locus *qSS7* associated with increased length and decreased width of rice seeds. *Theor. Appl. Genet.* **125**, 1717–1726 (2012).

20. Kirik, A., Ehrhardt, D.W. & Kirik, V. *TONNEAU2/FASS* regulates the geometry of microtubule nucleation and cortical array organization in interphase *Arabidopsis* cells. *Plant Cell* **24**, 1158–1170 (2012).

21. Lee, Y.K. *et al. LONGIFOLIA1* and *LONGIFOLIA2*, two homologous genes, regulate longitudinal cell elongation in *Arabidopsis*. *Development* **133**, 4305–4314 (2006).

22. Yan, X., Habedanck, R. & Nigg, E.A. A complex of two centrosomal proteins, CAP350 and FOP, cooperates with EB1 in microtubule anchoring. *Mol. Biol. Cell* **17**, 634–644 (2005).

23. Spinner, L. *et al.* A protein phosphatase 2A complex spatially controls plant cell division. *Nat. Commun.* **4**, 1863 (2013).

24. Sun, H. *et al.* Heterotrimeric G proteins regulate nitrogen-use efficiency in rice. *Nat. Genet.* **46**, 652–656 (2014).

25. Lu, Z. *et al.* Genome-wide binding analysis of the transcription activator ideal plant architecture1 reveals a complex network regulating rice plant architecture. *Plant Cell* **25**, 3743–3759 (2013).

26. Xie, K., Wu, C. & Xiong, L. Genomic organization, differential expression, and interaction of SQUAMOSA promoter-binding-like transcription factors and microRNA156 in rice. *Plant Physiol.* **142**, 280–293 (2006).

ONLINE METHODS

Plant materials and growing conditions. NIL-$GW7^{TFA}$ plants were generated by backcrossing the hybrid TFA × HJX74 line and further six times with HJX74. Contrasting allelic combinations of the $qGW7$ and $qGS3$ loci were assembled on the HJX74 background using NIL-$GS3$-$GW7^{TFA}$ and NIL-$gs3$-$gw7^{HJX74}$ plants[12]. Details of the germplasm used for the sequence diversity analysis have been provided elsewhere[12,24]. Field-grown NIL plants were raised in a rice paddy at an interplant spacing of 20 × 20 cm during the standard growing season at three experimental stations, located in Lingshui (Hainan Province), Hefei (Anhui Province) and Beijing. The primer sequences for the genotyping assays are provided in **Supplementary Table 7**.

Positional cloning of $qGW7$. Fine-scale mapping of $qGW7$ was based on 4,500 BC_3F_2 plants bred from the backcross between TFA and an *indica* variety, HJX74 (with HJX74 as the recurrent parent). The genomic DNA sequence in the $GW7$ candidate region was compared between TFA and HJX74. A list of the markers used for QTL analysis and positional cloning is given in **Supplementary Table 7**.

Transgene constructs. The $GW7$ coding sequence together with the 2-kb region upstream of the transcription start site and the 1-kb region downstream of the termination site was amplified from TFA and inserted into the pCAMBIA1300 vector (CAMBIA) to generate a p$GW7^{TFA}$∷$GW7^{TFA}$ expression cassette. A 406-bp cDNA fragment of $GW7$ was amplified from TFA and used to generate the p$Actin$∷RNAi-$GW7^{TFA}$ transgene. To construct the pUbi∷$gw7^{HJX74}$ vector, the HJX74 $GW7$ cDNA was amplified and inserted into the pUbi∷nos vector[24]. To construct p$GW7^{HJX74}$∷GUS, a 2-kb DNA fragment comprising the HJX74 $GW7$ promoter sequence was amplified and inserted into the pCAMBIA1301-GUS-nos vector[12]. Transgenic plants were generated by *Agrobacterium*-mediated transformation[27]. Relevant PCR primer sequences are given in **Supplementary Table 8**.

Quantitative RT–PCR analysis. Total RNA was extracted from plant tissues using TRIzol reagent (Invitrogen) and treated with RNase-free DNase I (Invitrogen) according to the manufacturer's protocol. To generate qRT-PCR template, the resulting RNA was reverse transcribed using the M-MLV Reverse Transcriptase kit (Promega). qRT-PCR was performed as described previously[28]; each qRT-PCR assay was replicated at least three times with three independent RNA preparations, and rice *Actin3* was used as a reference. Relevant PCR primer sequences are given in **Supplementary Table 8**.

ChIP-PCR assays. An ~2- to 3-g aliquot from 4-week-old transgenic pUbi∷Myc-$GW7$ rice plants was fixed by formaldehyde cross-linking and subjected to a ChIP assay based on an antibody to Myc (9E10, Santa Cruz Biotechnology) as described previously[29]. Enrichment of DNA fragments was determined using qRT-PCR analysis performed on three biological replicates. The relevant primer sequences are shown in **Supplementary Table 9**.

EMSA analysis. The $OsSPL16$ coding sequence was amplified from TFA and cloned into the pGEX-4T-1 vector (GE Healthcare). GST and GST-OsSPL16 fusion proteins were purified according to the manufacturer's protocol. DNA probes were amplified and labeled using a biotin labeling kit (Invitrogen). DNA gel shift assays were performed using the LightShift Chemiluminescent EMSA kit (Thermo Fisher Scientific). The relevant primer sequences are given in **Supplementary Table 10**.

Transactivation analysis. Transactivation analysis in rice protoplasts was performed as described elsewhere[30]. The 2-kb DNA fragment comprising the $GW7$ promoter was amplified from either TFA or HJX74 and used to generate reporter plasmids that contained the $GW7$ promoter and the luciferase gene. Full-length cDNA for $OsSPL16$ was amplified from HJX74, fused to the sequence encoding GAL4BD and inserted into pRT107 vector to generate the effector plasmid pRTBD-$OsSPL16$. Luciferase assays were performed as described elsewhere[30]. Relevant PCR primer sequences are given in **Supplementary Table 8**.

BiFC assays. The $GW7$ coding sequence was amplified form TFA and inserted into the pSY735 vector[31]. Full-length cDNAs for $OsTON1b$ and $OsTON2$ were amplified from TFA and subcloned into the pSY736 vector[31]. *Arabidopsis* protoplasts were prepared, transfected and visualized as described elsewhere[24]. Relevant PCR primer sequences are given in **Supplementary Table 8**.

Yeast one-hybrid assays. HJX74 $OsSPL16$ cDNA was inserted into the unique EcoRI and XhoI sites of the pB42AD vector (Takara). The 0.5-kb and 1.0-kb DNA fragments corresponding to the $GW7$ promoter were amplified from either TFA or HJX74 and subcloned into the pLacZi2μ vector[32] to drive *lacZ* reporter gene expression. The constructs were transformed into yeast strain EGY48; experimental procedures were performed according to the manufacturer's user guide. β-galactosidase activity was assayed by hydrolysis of *ortho*-nitrophenyl-β-D-galactopyranoside (ONPG), also measuring the absorbance for the released *ortho*-nitrophenyl (ONP) compound, on a spectrophotometer at 415 nm. Relevant PCR primer sequences are given in **Supplementary Table 8**.

Yeast two-hybrid assays. Yeast two-hybrid assays were performed as described elsewhere[24]. The full-length cDNAs for $OsTON1b$ and $OsTON2$ were amplified and subcloned into pGBKT7 vector (Takara), and the full-length $GW7$ coding sequence as well as sequences encoding N-terminal and C-terminal truncated deletions were inserted into the pGADT7 vector (Takara). The vectors were transformed into yeast strain AH109. The GW7 protein was used as bait to screen a cDNA library prepared from equal amounts of poly(A)-containing RNAs from various rice samples, including seedlings, roots, leaves, stems and young panicles, among others. Experimental procedures for screening and plasmid isolation were performed according to the manufacturer's user guide. Primer sequences are provided in **Supplementary Table 8**.

27. Huang, X. *et al.* Natural variation in the *DEP1* locus enhances grain yield in rice. *Nat. Genet.* **41**, 494–497 (2009).
28. Jiang, C. *et al.* Root architecture and anthocyanin accumulation of phosphate starvation responses are modulated by the GA-DELLA signaling pathway in *Arabidopsis*. *Plant Physiol.* **145**, 1460–1470 (2007).
29. Gendrel, A.V. *et al.* Profiling histone modification patterns in plants using genomic tiling microarrays. *Nat. Methods* **2**, 213–218 (2005).
30. Chern, M. *et al.* A rice transient assay system identifies a novel domain in NRR required for interaction with NH1/OsNPR1 and inhibition of NH1-mediated transcriptional activation. *Plant Methods* **8**, 6 (2012).
31. Bracha-Drori, K. *et al.* Detection of protein-protein interactions in plants using bimolecular fluorescence complementation. *Plant J.* **40**, 419–427 (2004).
32. Li, G. *et al.* Coordinated transcriptional regulation underlying the circadian clock in *Arabidopsis*. *Nat. Cell Biol.* **13**, 616–622 (2011).